New concepts for Reynolds stress transport equation modeling of inhomogeneous flows

By J. Blair Perot AND Parviz Moin

1. Motivation and objectives

The ability to model turbulence near solid walls and other types of boundaries is important in predicting complex engineering flows. Most turbulence modeling has concentrated either on flows which are nearly homogeneous or isotropic, or on turbulent boundary layers. Boundary layer models usually rely very heavily on the presence of mean shear and the production of turbulence due to that mean shear. Most other turbulence models are based on the assumption of quasi-homogeneity. However, there are many situations of engineering interest which do not involve large shear rates and which are not quasi-homogeneous or isotropic. Shear-free turbulent boundary layers are the prototypical example of such flows, with practical situations being separation and reattachment, bluff body flow, high free-stream turbulence, and free surface flows. Although these situations are not as common as the variants of the flat plate turbulent boundary layer, they tend to be critical factors in complex engineering situations.

The models developed in this work are intended to extend classical quasi-homogeneous models into regions of large inhomogeneity. These models do not rely on the presence of mean shear or production, but are still applicable when those additional effects are included. Although the focus will be on shear-free boundary layers as tests for these models, results for standard shearing boundary layers will also be shown.

Eddy viscosity models and k-ϵ type models are fundamentally incapable of representing shear-free boundary layers. They assume that there exists a proportionality between the turbulent stresses and the mean shear. This clearly can not be the case in a shear-free flow. The next level of turbulence modeling, Reynolds stress transport equation models, are the simplest type of model capable of capturing the shear-free or nearly shear-free situation.

The models developed in this work are based on our studies of the near wall behavior of turbulence in shear-free boundary layers (Perot & Moin, 1993). These studies of shear-free turbulent boundary layers have provided a physical understanding of the wall/turbulence interaction, and it is the goal of this paper to translate this physical understanding into improved near wall turbulence models. The inclusion of more physics into the models presented herein allows us to obtain better agreement with direct numerical simulation (DNS) data without resorting to additional model constants, *ad hoc* damping functions, or imposed near wall behaviors.

2. Dissipation model

2.1 Introduction

In the following section, some advances in near wall dissipation modeling are presented. What is described is not so much a new model, but a technique for extending classical (quasi-homogeneous) dissipation models into the near wall region. Unlike previous techniques which were ultimately *ad hoc* in nature, this model for the near wall dissipation is based on a simple mathematical decomposition and physical observations of the behavior of near wall turbulence.

The physical inspiration for the dissipation model is found in figure 1. This figure is from simulations of a shear-free solid wall (Perot & Moin, 1993). In these simulations, a solid wall (no-slip boundary conditions) is suddenly inserted into isotropic, homogeneous decaying turbulence. The wall interacts with the turbulence, creating a boundary layer in the turbulent statistics which grows into the turbulence as time progresses. The figure shows two planes parallel to the solid wall plotted with contours of the instantaneous tangential velocity. The top plane is far from the wall, and the min/max values of the contours correspond to *rms* intensities that are very close to their free-stream value. The bottom plane is much closer to the wall and has much smaller min/max levels (and *rms* intensities). The crucial observation from these figures is that the structure of the turbulence in the two planes is very similar (i.e., the location of the contours), while the magnitude or scale of the turbulent fluctuations (measured either by the min/max of the contours or by the *rms* intensities) differs by an order of magnitude from one plane to the other. The distance over which the turbulent intensities are damped by the wall is much smaller than the distance over which the eddy structure (as measured by the eye) changes appreciably. This implies that in very near wall turbulence, there is a separation of scales, with the turbulent intensities changing much more rapidly than variations in the actual eddy structure. These observations should also apply in the near wall region of standard flat plate boundary layers. Whether they apply in even more complicated situations is not important since this is the inspiration, not the foundation, for the dissipation tensor model.

The decomposition of turbulence into a turbulent intensity component and a turbulent structure component can be accomplished mathematically in the following way.

$$u_i = \overline{Q}_{ip}\tilde{u}_p. \tag{1}$$

Here, u_i is the fluctuating velocity, $\overline{Q}_{ip}$ is a generalized turbulent intensity, and $\tilde{u}_p$ is the velocity structure. This operation can also be thought of as a mapping or a transformation which scales the fluctuating velocity component, so that the resultant statistical quantity, $\tilde{u}_p$, is a nearly homogeneous quantity. Several appropriate choices for $\overline{Q}_{ip}$ which accomplish this goal will be discussed in Section 2.3. However, at this point it is sufficient to observe that equation (1) is a mathematical decomposition, which is well defined as long as $\overline{Q}_{ip}$ is an invertible matrix.

The turbulent intensity, $\overline{Q}_{ip}$, has an overbar to indicate that it is considered to be a statistical average of turbulence quantities and a known quantity. Mathematically,

Min = −.17
Max = .21

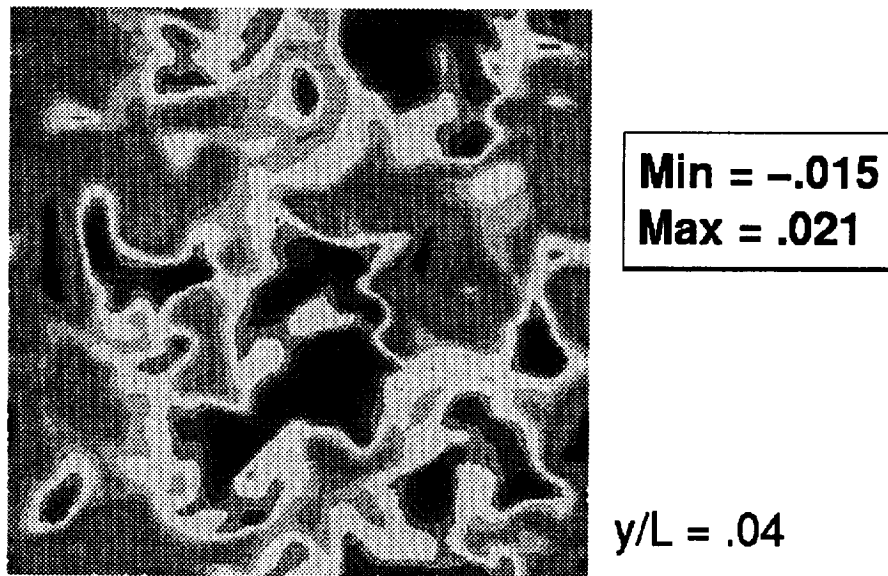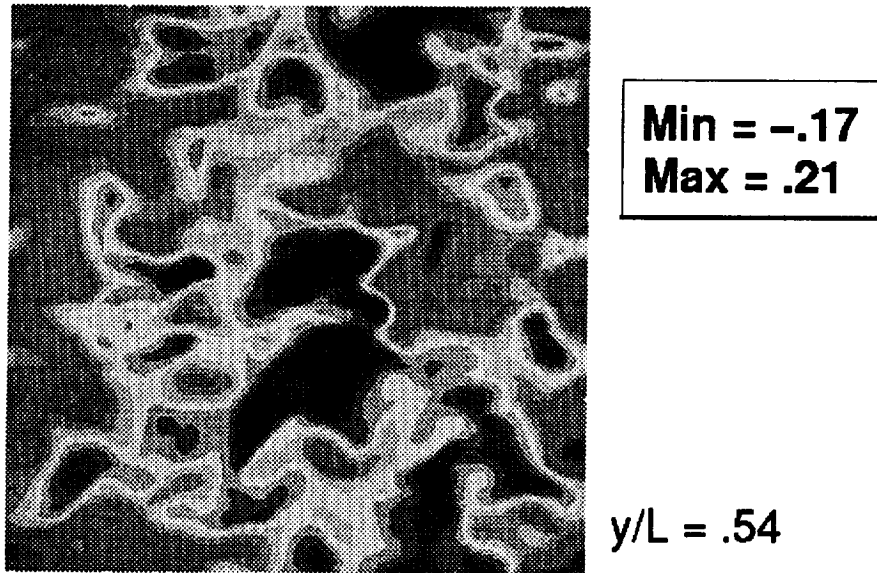y/L = .54

Min = −.015
Max = .021

y/L = .04

FIGURE 1. Contours of instantaneous tangential velocity in planes parallel to a shear-free solid wall. ($Re_T = 134$)

the definition of $\overline{Q}_{ip}$ is arbitrary, but physically, it is important to choose a definition for $\overline{Q}_{ip}$ which reflects its intended function as a measure of the turbulent intensity. Different definitions for $\overline{Q}_{ip}$ produce models of varying complexity and accuracy. In the context of this work, two definitions for $\overline{Q}_{ip}$ will be considered. One definition is based on the turbulent kinetic energy and the other definition is based on the Reynolds stress tensor. Better definitions for $\overline{Q}_{ip}$ tend to produce better models at the price of increased complexity.

Having chosen a definition for the turbulent intensity, the properties of the velocity structure can then be derived from equation 1. The velocity structure (unlike the turbulent intensity tensor) retains the random spatial and temporal fluctuations of the original velocity field. The velocity structure can, in a sense, be thought of as a normalized fluctuating velocity scaled by the generalized turbulent intensity tensor. The result of this normalization by the turbulent intensity is that the velocity structure becomes a homogeneous, or at least a quasi-homogeneous, turbulence quantity. It now becomes possible to think of the decomposition (equation 1) as a splitting of turbulence into "homogeneous" factor (velocity structure) and "inhomogeneous" factor (turbulent intensity).

An analogy with Reynolds decomposition into mean and fluctuating velocities can be made. However, in this case, the decomposition is multiplicative rather than additive, and rather than subtracting off the mean to get to fluctuating velocity, we are dividing by some turbulent intensity to get the velocity structure. The unknown turbulent quantity of interest (the velocity structure) now has zero mean and unity (or nearly unity) variance.

2.2 Mathematical details

The result of substituting this mathematical decomposition (equation 1) into the definition for the homogeneous dissipation tensor,

$$\epsilon_{ij} \equiv 2\nu\overline{u_{i,p}u_{j,p}}, \tag{2}$$

is

$$\frac{\epsilon_{ij}}{2\nu} = \overline{Q}_{im,p}\left(\overline{\tilde{u}_m\tilde{u}_n}\right)\overline{Q}_{jn,p} + \overline{Q}_{im}(\overline{\tilde{u}_{m,p}\tilde{u}_{n,p}})\overline{Q}_{jn}$$

$$+ \frac{1}{2}\left(\overline{Q}_{im,p}(\overline{\tilde{u}_m\tilde{u}_n}),_p\overline{Q}_{jn} + \overline{Q}_{im}(\overline{\tilde{u}_m\tilde{u}_n}),_p\overline{Q}_{jn,p}\right) \tag{3}$$

$$+ \frac{1}{2}\left(\overline{Q}_{im,p}W_{mnp}\overline{Q}_{jn} - \overline{Q}_{im}W_{mnp}\overline{Q}_{jn,p}\right)$$

where the tensor $W_{mnp} = (\overline{\tilde{u}_m\tilde{u}_{n,p}} - \overline{\tilde{u}_{m,p}\tilde{u}_n})$ is antisymmetric in m and n.

This expression for the dissipation tensor splits the dissipation into three fundamental parts: the dissipation due to spatial variations in the turbulent intensity (first term on the right hand side), the dissipation due to spatial variations in the turbulent structure (second term on the right hand side), and coupling terms representing the interaction of the first two dissipation terms with each other (last two terms on the right hand side).

The contribution to the dissipation due to variations in the turbulent intensity (first term on the right hand side) dominates in regions of large inhomogeneity where the turbulent intensity changes rapidly. This "inhomogeneity term" depends only on the turbulent intensity tensor and the Reynolds stress tensor (by definition, $\overline{\tilde{u}_m \tilde{u}_n} = \overline{Q}_{mi}^{-1} R_{ij} \overline{Q}_{jn}^{-1}$ where $R_{ij} = \overline{u_i u_j}$). The generalized turbulent intensity, $\overline{Q}_{ij}$, is assumed to be well defined in terms of other quantities available in the closure, so the inhomogeneity term does not need to be modeled. Because equation 3 is an exact expression, the inhomogeneity term can also be thought of as an "exact term". In regions where the inhomogeneity term dominates (such as near walls), equation 3 will give exact results for the dissipation.

The second term on the right hand side of equation 3 involves a statistical quantity which will be called the structure dissipation tensor. This quantity is much easier to model than the dissipation tensor itself because the velocity structure is, in fact,quasi-homogeneous. Therefore, models based on the assumption of quasi-homogeneity (i.e. most classical dissipation tensor models) can be expected to work very well for this quantity.

The two coupling terms can be thought of as redistribution terms. Depending on the definition of $\overline{Q}_{ij}$, they either are identically zero or their trace is zero. The separation of scales between variations in the turbulent structure (with length scales on the order of the large eddy length scale) and variations in the turbulent intensity (with much smaller length scales on the order of $\sqrt{\nu t}$) suggests that the coupling terms should be relatively small; typically, processes which occur at different scales tend to have little interaction. The exact nature of these terms will be further investigated when specific expressions for $\overline{Q}_{ij}$ are examined.

2.3 Dissipation model

There are a number of choices that can be made for the generalized turbulent intensity tensor, $\overline{Q}_{ij}$. A simple choice is an isotropic scale tensor proportional to the square root of the turbulent kinetic energy, $\overline{Q}_{ij} = k^{1/2}\delta_{ij}$, where k is the turbulent kinetic energy. The resulting expression for the dissipation then becomes

$$\frac{\epsilon_{ij}}{2\nu} = (k^{1/2})_{,p}(k^{1/2})_{,p}\frac{R_{ij}}{k} + \frac{1}{2}(k)_{,p}\left(\frac{R_{ij}}{k}\right)_{,p} + k\overline{\tilde{u}_{i,p}\tilde{u}_{j,p}} \tag{4}$$

This equation is attractive because of its simplicity. The only term requiring modeling is the velocity structure dissipation, $\tilde{\epsilon}_{ij} = 2\nu\overline{\tilde{u}_{i,p}\tilde{u}_{j,p}}$. The inhomogeneity term and redistribution term (the first and second terms on the right hand side) are well defined, and in the sense described previously, they are "exact". Despite its attractiveness, this model suffers from some basic flaws. In particular, it is only weakly realizable; the kinetic energy is guaranteed to remain positive when using this model, but the Reynolds stress tensor itself may become indefinite.

A more attractive dissipation model can be obtained by using a slightly more complicated choice for the velocity scale tensor given by $\overline{Q}_{im}\overline{Q}_{mj} = R_{ij}$. This makes $\overline{Q}_{ij}$ the square root of the Reynolds stress tensor. Because R_{ij} is positive definite, this square root is well defined (up to a plus or minus sign on each eigenvalue, which

can be arbitrarily chosen). Note that $\overline{Q}_{ij}$ has the same eigenvectors as R_{ij} with eigenvalues that are the square root of the eigenvalues of R_{ij}. $\overline{Q}_{ij}$ is, therefore, a symmetric tensor like R_{ij}. This definition is a natural generalization of the definition used to derive equation 4. The sign of the square root is not important in the model because all terms involving the generalized intensity appear in pairs, canceling out any dependence on the sign. Note that with this definition $\overline{\tilde{u}_i \tilde{u}_j} = \delta_{ij}$, indicating that the velocity structure is very close to a homogeneous isotropic quantity.

With this enhanced choice for the turbulent intensity tensor, the expression for the dissipation takes the form

$$
\begin{aligned}
\epsilon_{ij} = {} & 2\nu \overline{Q}_{im,p}\overline{Q}_{jm,p} + \overline{Q}_{im}\tilde{\epsilon}_{mn}\overline{Q}_{nj} \\
& + \nu\left(\overline{Q}_{im,p}W_{mnp}\overline{Q}_{nj} - \overline{Q}_{im}W_{mnp}\overline{Q}_{nj,p}\right).
\end{aligned}
\tag{5}
$$

where $\tilde{\epsilon}_{mn} = 2\nu\overline{\tilde{u}_{i,p}\tilde{u}_{j,p}}$ is again the velocity structure dissipation tensor.

The first two terms of equation 5 are the now familiar inhomogeneous and homogeneous dissipation terms. The third term of equation 5 acts as a redistribution term and is particularly interesting. It is zero if the Reynolds stress tensor is either isotropic or homogeneous. In fact, it is zero if $Q_{im,p} = sQ_{im}$ where s is a scalar quantity. This turns out to be the case in spatially decaying turbulence if there is no return to isotropy in the sense of Lumley (1978). So in some sense, this term can also be thought of as a return to isotropy term.

Further insight into the redistribution term can be gained by evaluating the Reynolds stresses in their principal coordinates. Then Q_{ij} is a diagonal tensor with $Q_{\alpha\alpha} = R_{\alpha\alpha}^{1/2}$ (here and throughout the text, no summation is implied for Greek indices). In this arrangement, the redistribution term only contributes to the off-diagonal components of the dissipation tensor; hence, it is a coupling or redistribution term. It is partly responsible for enabling the dissipation tensor to have principal axes that differ from those of the Reynolds stress tensor. This is a useful property of the model, but one which is burdensome because the tensor W_{mnk} introduces nine new unknowns for which no model (even quasi-homogeneous) now exists. In what follows, the terms involving W_{mnk} will be neglected. In the tests that have been performed, this simplification does not appear to affect the performance of the model significantly and, therefore, appears to be warranted.

2.4 Mathematical constraints

It can be shown that every component of this model has the correct leading (and often higher order) terms in a Taylor series expansion about a no-slip wall. This non-trivial result holds irrespective of the model for the structure dissipation as long as the structure dissipation approaches a constant near the wall. It is a result of the fact that inhomogeneity dominates in the near wall region, and the inhomogeneous term of equation 5 is exact.

It is important that models have the correct asymptotic behavior as they approach the wall (Launder & Reynolds, 1983). For instance, at a solid wall the transverse components of the dissipation (ϵ_{11} and ϵ_{33}) must exactly balance the corresponding

diffusion components, or turbulence will spuriously be created by the wall. Some dissipation models (see Lai & So, 1990) have the asymptotic behavior for a no-slip wall imposed upon them. These models will probably fail when presented with any other type of boundary such as a free surface, a transpiring wall, etc. This is not the case for the current model, which does not impose asymptotic behavior, but which obtains correct asymptotic behavior (in numerous flow situations) by virtue of the "exact" inhomogeneous term.

This model also satisfies certain mathematical constraints. By its construction, the model is Galilean and tensorally invariant. It can be seen from equation 5 (with $W_{mnk} = 0$) that if the structure dissipation tensor is positive definite, then the dissipation tensor can also be guaranteed to be positive definite. Strict realizability (Schumann, 1977) in the low Reynolds number limit can be shown by analyzing the viscous terms. In principal coordinates, the sum of the viscous diffusion term, $D_{ij} = \nu R_{ij,kk}$, and dissipation term becomes

$$-\epsilon_{\alpha\alpha} + D_{\alpha\alpha} = 2\nu R_{\alpha\alpha}^{1/2} R_{\alpha\alpha,pp}^{1/2} - R_{\alpha\alpha}\tilde{\epsilon}_{\alpha\alpha} \tag{6}$$

Therefore, when the Reynolds number is low, the following expression can be written, $(R_{\alpha\alpha}^{1/2})_{,t} = \nu(R_{\alpha\alpha}^{1/2})_{,mm} - \frac{\epsilon_{\alpha\alpha}}{2} R_{\alpha\alpha}^{1/2}$. This indicates that the turbulent intensities diffuse and decay exponentially in time, which, along with equation 6, guarantees that the Reynolds stress tensor can not become indefinite as time advances.

2.5 Results

Two classical models for the homogeneous dissipation tensor assume that dissipation is isotropic, ($\epsilon_{ij}^{I} = \frac{2}{3}\epsilon\delta_{ij}$), or that the dissipation is proportional to the Reynolds stress tensor (Rotta, 1951), ($\epsilon_{ij}^{R} = \frac{\epsilon}{k}R_{ij}$). Figures 2a and 2b show comparisons of these two models with the direct numerical simulation (DNS) data of Perot & Moin (1993) for flow near a shear-free solid wall. It is evident that the isotropic assumption works well far from the wall and the "low Reynolds number" Rotta model works well close to the wall. An improved near wall dissipation model can, therefore, be constructed using a combination of these two classical models. A number of mixed models of this type exist, each differing in the choice of parameter which is used to blend the two models.

To demonstrate the possible improvement, a mixed model is also presented in figures 2a and 2b. The parameter $A = 1 - \frac{9}{8}(a_{mn}a_{nm} - a_{mp}a_{pn}a_{nm})$ (Tselepidakis, 1991), where $a_{ij} = R_{ij}/k - 2/3\delta_{ij}$ is the non-dimensional Reynolds stress anisotropy tensor, is used to blend the two models. A is 1 in isotropic turbulence and zero in the two component limit that occurs at a wall. The mixed model is then written as

$$\epsilon_{ij}^{M} = A\frac{2}{3}\epsilon\delta_{ij} + (1 - A)\frac{\epsilon}{k}R_{ij} \tag{7}$$

An expression very similar to the mixed model will also be used to model the structure dissipation tensor in the inhomogeneity-capturing model,

$$\tilde{\epsilon}_{ij} = \frac{\tilde{\epsilon}}{k}\left(A\frac{2}{3}\delta_{ij} + (1 - A)\frac{R_{ij}}{k}\right) \tag{8}$$
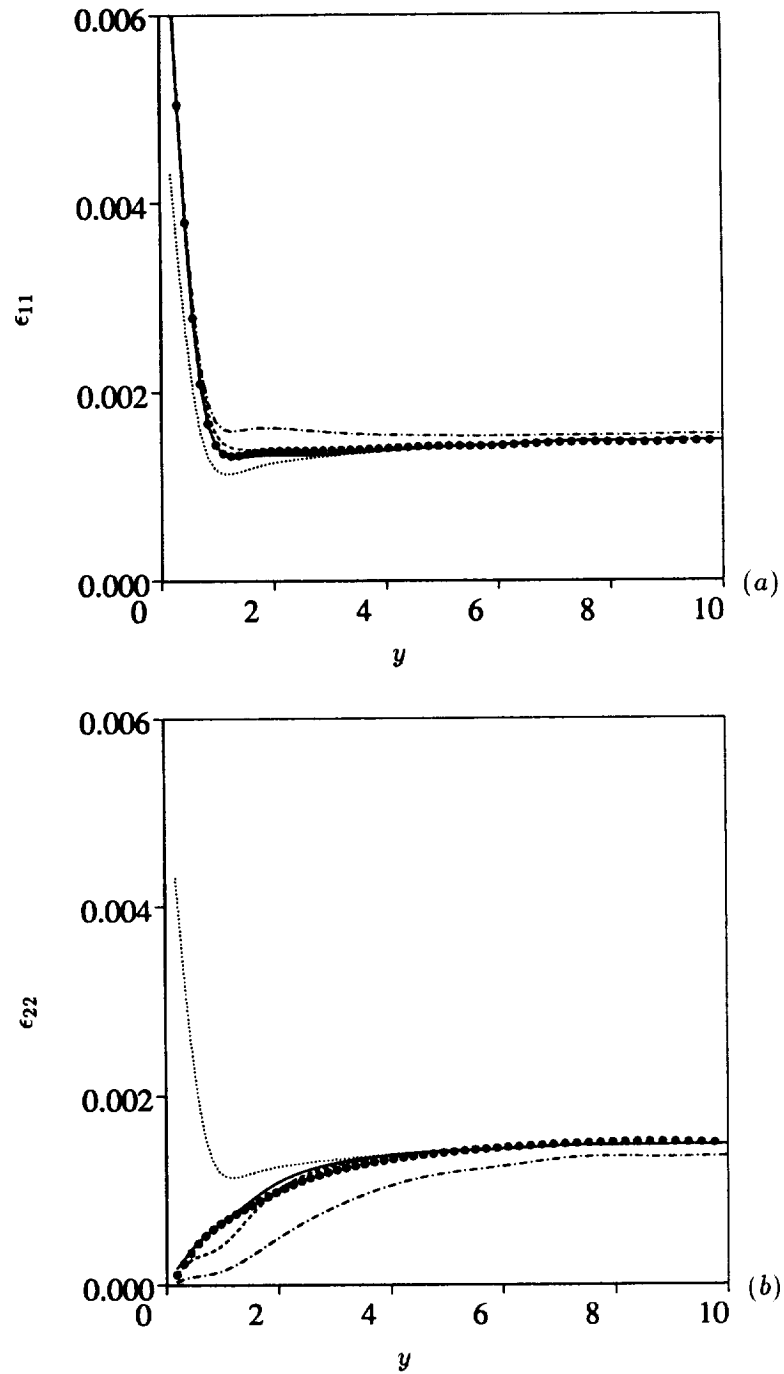
FIGURE 2.   Dissipation near a shear-free solid wall. $(Re_T = 54)$, (a) Tangential dissipation, (b) Normal dissipation.   ● , DNS data; ········ , Isotropic model; —·— , Rotta model; ---- , mixed model; ——— , inhomogeneity model.
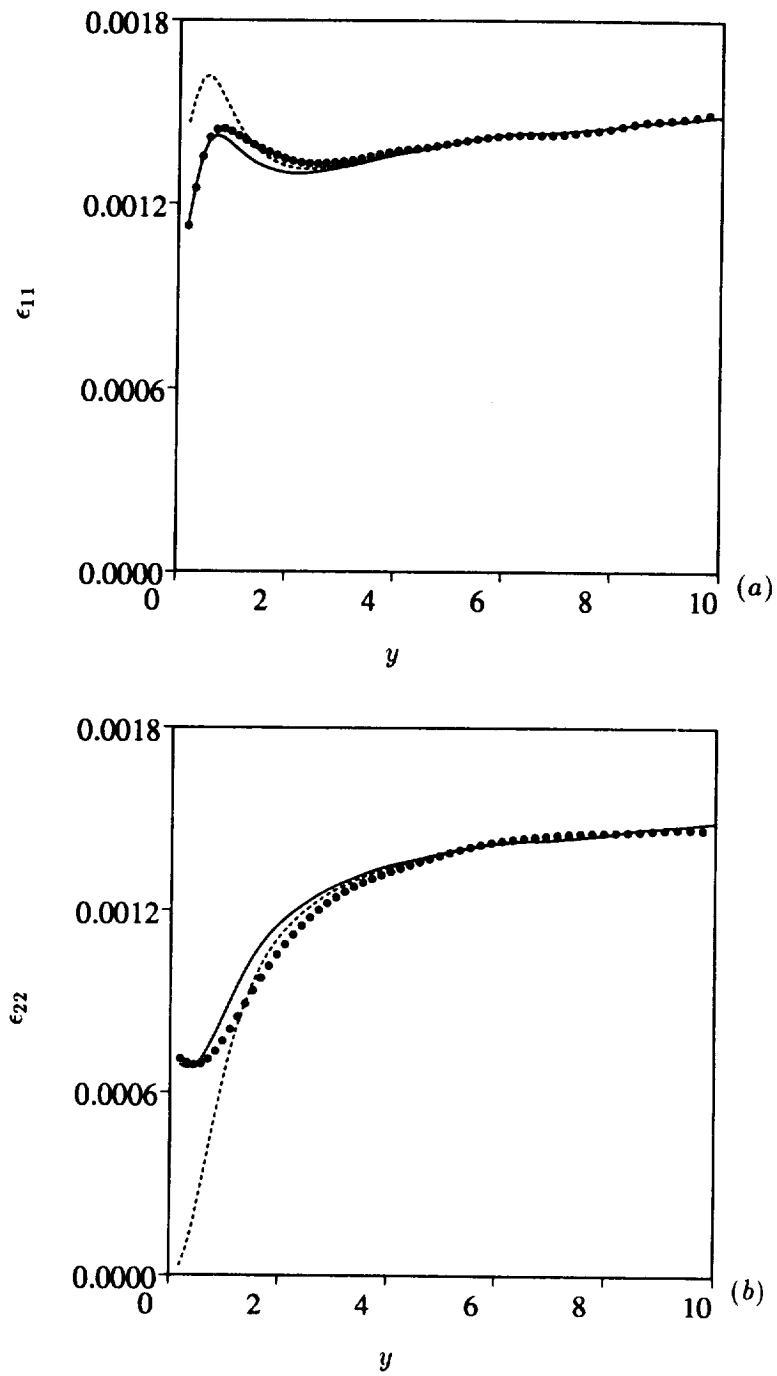
FIGURE 3. Dissipation near a free surface. (Re_T = 54), (a) Tangential dissipation, (b) Normal dissipation. ● , DNS data; - - - - , mixed model; ———— , inhomogeneity model.

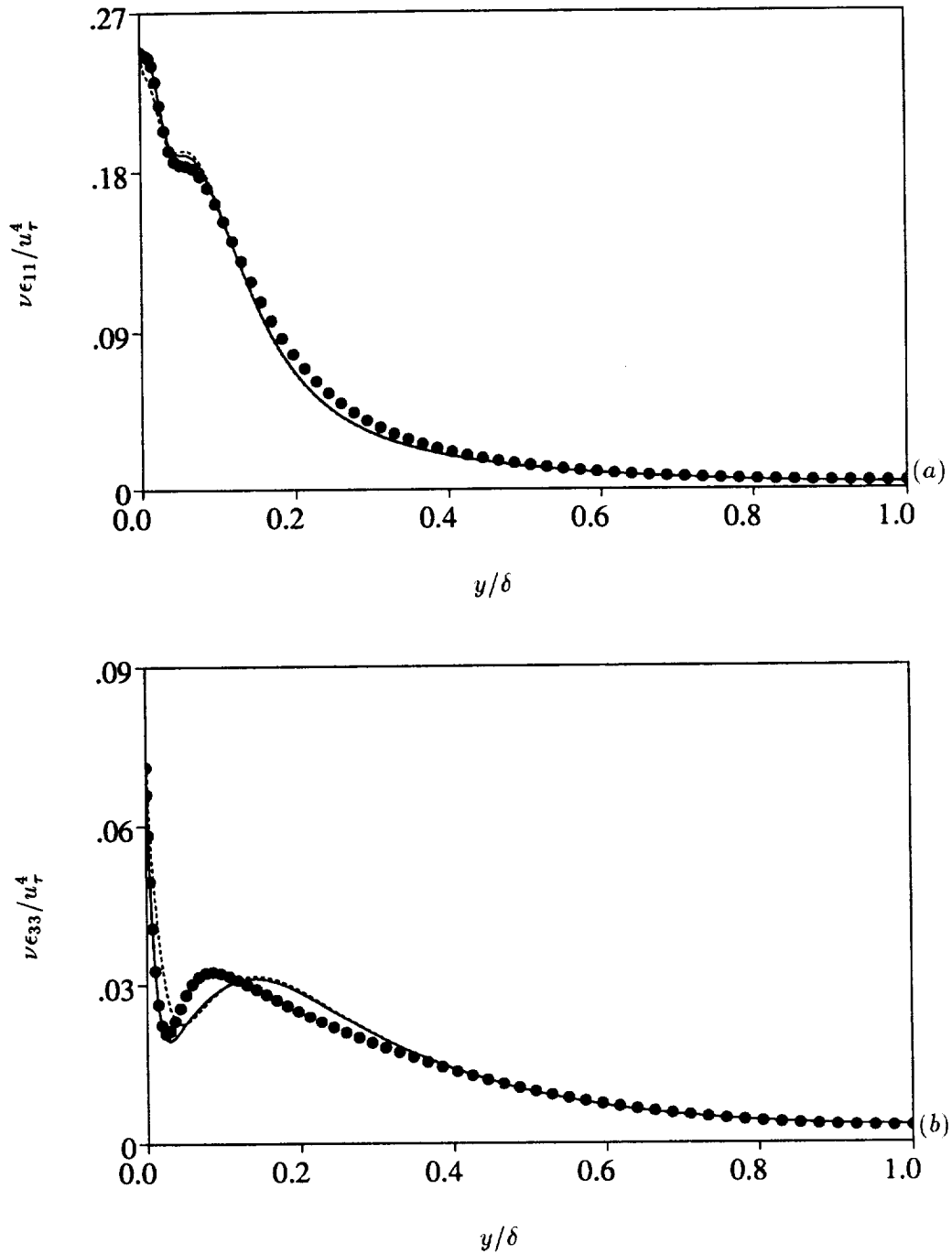FIGURE 4. Dissipation in turbulent channel flow. (a) Streamwise dissipation, (b) Spanwise dissipation.   • , DNS data of Mansour, Kim, & Moin (1988); - - - - , mixed model; ———— , inhomogeneity model.
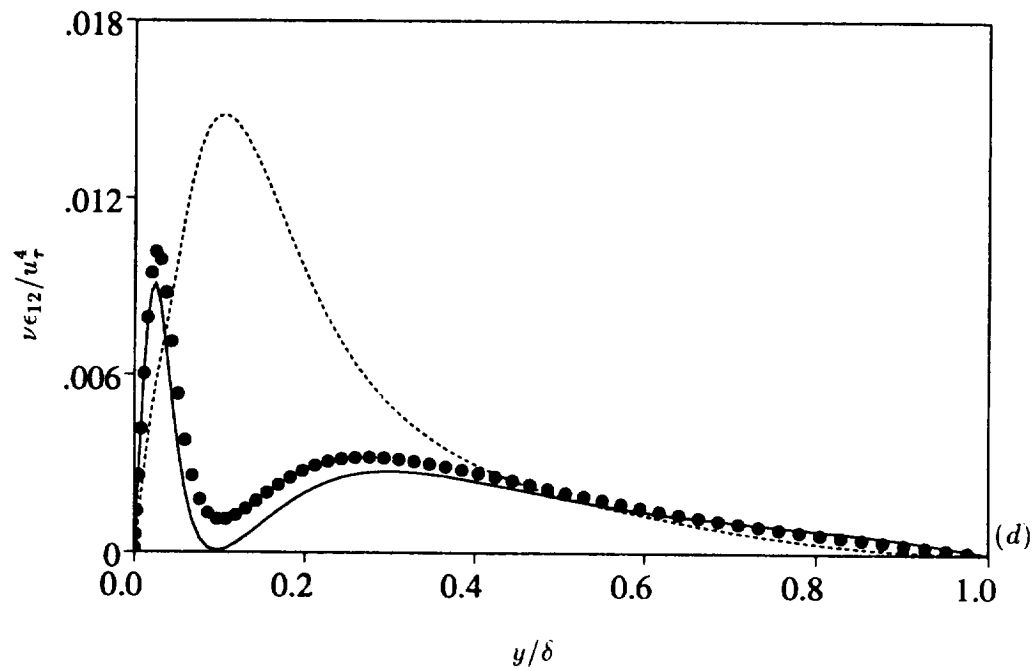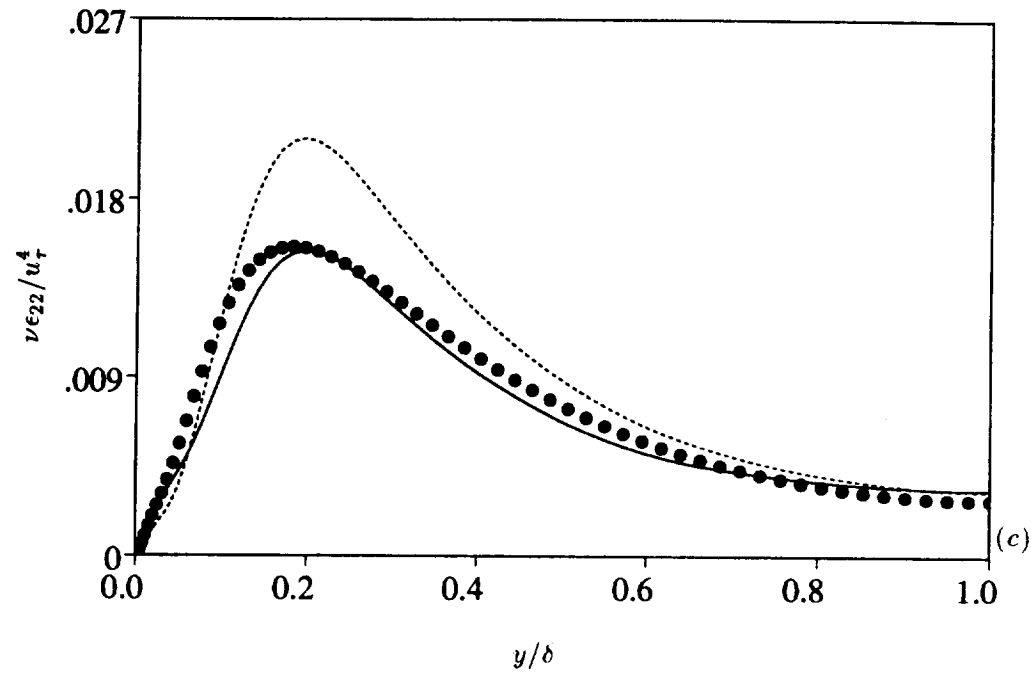
FIGURE 4. (Cont.) Dissipation in turbulent channel flow. (c) Normal dissipation, (d) Shear stress dissipation. ● , DNS data of Mansour, Kim, & Moin (1988); ---- , mixed model; ——— , inhomogeneity model.

where $\tilde{\epsilon}$ is (in analogy with the dissipation) one half of the trace of the structure dissipation tensor. Equation 5 with equation 8 and $W_{ijk} = 0$ gives the full inhomogeneity capturing model for the dissipation tensor,

$$\epsilon_{ij}^I = 2\nu \overline{Q}_{im,p}\overline{Q}_{jm,p} + \tilde{\epsilon}\left(\frac{2}{3}A\frac{R_{ij}}{k} + (A-1)\frac{R_{im}R_{mj}}{k^2}\right). \tag{9}$$

Note that in the mixed model ϵ must be specified. In the inhomogeneity model, $\tilde{\epsilon}$ must be specified. In the tests of the models, these quantities will be supplied from the direct numerical simulation (DNS) data, but in an actual modeling situation, they would have to be derived in some other manner (usually from a dissipation transport equation). The quantity $\tilde{\epsilon}$ is probably easier to arrive at (since it is much smoother than ϵ). In addition, $\tilde{\epsilon}$ has less effect on the overall model performance because the terms involving $\tilde{\epsilon}$ are small near the wall. The inhomogeneity model is also shown in figures 2a and 2b. It falls almost exactly on the DNS data.

Both the mixed model and the inhomogeneity model work well for the case of a shear-free solid wall. A better test of the two models' ability to handle inhomogeneity is presented in figures 3a and 3b where DNS data, the mixed model, and the inhomogeneity model are shown for the case of turbulence next to a free surface. The mixed model gives an incorrect value at the surface for the tangential dissipation and completely inappropriate behavior for the normal dissipation component. The inhomogeneity model, on the other hand, closely follows the DNS data and gives particularly good far field and near surface behaviors.

The final test of the model is presented in figures 4a-d. This shows the case of fully developed channel flow. The data is from Mansour, Kim & Moin (1988). Both models work well for the streamwise component of the dissipation. The inhomogeneity model captures the function value *and* the slope exactly at the wall. The spanwise components of the models behave very similarly, with the inhomogeneity model showing an improvement in the slope at the wall. However, the mixed model severely overestimates the normal dissipation and does not have the correct qualitative behavior for ϵ_{12}.

2.6 Summary

A new modeling technique for extending classical dissipation models into regions of large inhomogeneity has been developed. It is based on a hypothesis of separation of scales and derived from a simple mathematical decomposition. This decomposition uses the the square root of the Reynolds stress tensor as a generalized turbulent intensity to transform (or map) the fluctuating velocity into a quasi-homogeneous quantity (the velocity structure). The resulting inhomogeneity model, derived from this decomposition, satisfies all known mathematical constraints and is relatively simple to implement. It has been shown that the model gives superior results in both wall and surface bounded flows. The formalism developed here has also been applied to modeling of the scalar dissipation and heat flux dissipation (Malan, 1993) with equally impressive results.

3. Pressure-strain model

3.1 Introduction

The pressure-strain term is an inter-component energy redistribution term; it causes no net change in the total kinetic energy. Experiments on homogeneous turbulence (Lumley & Newman, 1977) show that this redistribution by the pressure-strain (at least by the nonlinear (slow) part of the pressure-strain) tends to result in a return to isotropy. The logical assumption from this observation is that the pressure-strain term is driven by the non-dimensional anisotropy in the Reynolds stresses, $a_{ij} = R_{ij}/k - 2/3\delta_{ij}$, which by construction is a trace free tensor, like the pressure-strain.

Almost all models for the pressure-strain are based on the assumption that the pressure-strain must be a function of the anisotropy tensor. The models of Rotta (1951), Shih & Lumley (1985), and Speziale, Sarkar and Gatski (1991), are examples of models of this type. Some of these models are very complicated, but none produce truly convincing results. In fact, Reynolds (1988) has shown that any pressure-strain model based on this assumption is incapable of capturing the effects of rapid rotation. Any model of this type is also incapable of predicting a flow where the boundary condition on the tangential velocity changes suddenly, such as the sudden insertion of a permeable wall (Perot & Moin, 1993) or the sudden change from a solid wall to a free surface boundary condition. In those situations, the pressure-strain term changes instantaneously, whereas the Reynolds stress and anisotropy tensors take some time to evolve.

Furthermore, return to isotropy cannot be the driving mechanism for the pressure-strain term near a free surface or a solid wall. In such cases, the tangential stresses are larger than the normal stresses, and yet there is still a transport of energy to the tangential stresses. In many near wall flows, the pressure-strain term actually enhances anisotropy. In the face of all this evidence, it seems clear that the very assumptions upon which pressure-strain modeling are based need to be reevaluated.

3.2 Modeling

The physical model for turbulent flow proposed in Perot & Moin (1994a) is a useful guide to pressure-strain modeling. In that model, it is assumed that in any turbulent flow there are opposing events. These events will tend to balance each other (resulting in zero net transfer of energy) unless one of the events is weaker than the other. In the near wall case, antisplats (blobs of fluid moving away from the boundary) are weaker due to the fact that tangential energy is removed by dissipation near the wall. This limits the antisplat's ability to convert tangential energy into normal energy. In homogeneous turbulence, the situation is somewhat different: if one component of the turbulence is less energetic than the others then it will not be able to deliver energy to the other components as effectively. This will result in a net transfer of energy into the less energetic component and a return to isotropy.

In the near wall case, dissipation and diffusion control intercomponent energy

transfer by determining the imbalance between splats and antisplats. In homogeneous turbulence, Reynolds stresses anisotropy controls energy transfer. To translate these ideas into a model, it is instructive to look at the evolution equation for the non-dimensional anisotropy. In unsheared homogeneous turbulence, the exact equation for the non-dimensional anisotropy tensor is

$$a_{ij,t} = \frac{\Pi_{ij}}{k} + \frac{\epsilon}{k}(\frac{r_{ij}}{k} - \frac{e_{ij}}{\epsilon}) \tag{10}$$

where $r_{ij} = R_{ij} - \frac{2}{3}k\delta_{ij}$ and $e_{ij} = \epsilon_{ij} + \frac{2}{3}\epsilon\delta_{ij}$ are the dimensional anisotropy of the Reynolds stress and dissipation tensors, Π_{ij} is the pressure-strain tensor, and $a_{ij} = R_{ij}/k - 2/3\delta_{ij}$ is the nondimensional Reynolds stress anisotropy tensor. Note that typically the dissipation is more isotropic than the Reynolds stresses (due to quasi-isotropy in the smallest scales of motion), so the second term on the right hand side of the equation tends to increase anisotropy. For return to isotropy to occur, the pressure-strain must be large enough to drive the overall right hand side negative. A reasonable model for the pressure-strain is, therefore, that the pressure strain is proportional to the right hand side,

$$\Pi_{ij} = -C_\pi(-e_{ij} + \frac{\epsilon}{k}r_{ij}) \tag{11}$$

where $C_\pi > 1$ will guarantee return to isotropy in homogeneous turbulence.

This model has the attractive property that it behaves appropriately as a function of Reynolds number. At very high Reynolds numbers, dissipation becomes isotropic, and the standard return to isotropy model (of Rotta) is recovered. At low Reynolds numbers, the approximation $\epsilon_{ij} = \frac{\epsilon}{k}R_{ij}$ (Rotta, 1951) becomes increasingly accurate, so $e_{ij} = \frac{\epsilon}{k}r_{ij}$ at low Reynolds numbers, and the model approaches zero in the low Reynolds number limit. Therefore, at low Reynolds numbers there is no return to isotropy, a property which was proposed by Lumley (1978) and observed in simulations performed by Hallback & Johansson (1992).

To use this model in inhomogeneous flows, it must be generalized. Instead of $-e_{ij}$, the quantity $-e_{ij} + d_{ij}$ will be used; $d_{ij} = \nu r_{ij,mm}$ is the anisotropy in the viscous diffusion term, which is zero in homogeneous turbulence. In addition, the inverse time scale $\frac{\epsilon}{k}$, is not correct near a wall. It is replaced by $A\frac{\epsilon}{k}$ where A is the flatness parameter described earlier in the section on dissipation modeling. A is 1 in isotropic turbulence and 0 at a wall. This accounts for the fact that in the two component limit near a wall, classical return to isotropy is not expected. The model for the pressure-strain then becomes

$$\Pi_{ij} = -C_\pi(-e_{ij} + \nu r_{ij,mm} + A\frac{\epsilon}{k}r_{ij}) \tag{12}$$

As the next section will show, this model gives reasonable behavior in shear-free boundary layers. Since the development given here is essentially for the nonlinear (slow) pressure-strain, these shear-free flows are appropriate situations in which to test the model.
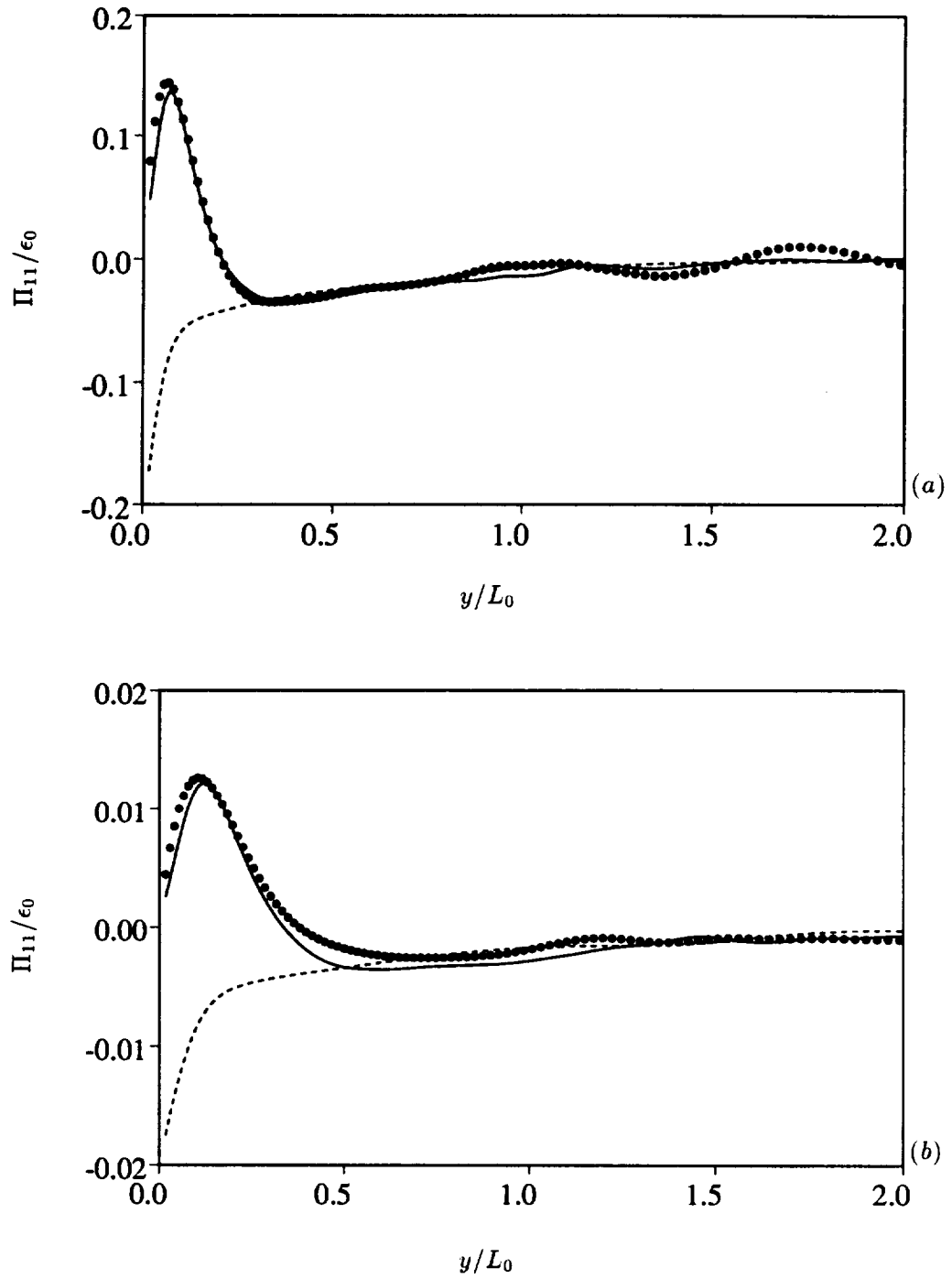
FIGURE 5. Pressure-strain near a shear-free wall. ($Re_T = 134$),   (a) $t/T_0 = 1.0$, (b) $t/T_0 = 4.5$.   ● , DNS data; - - - - , Rotta model; ———— , Present model.
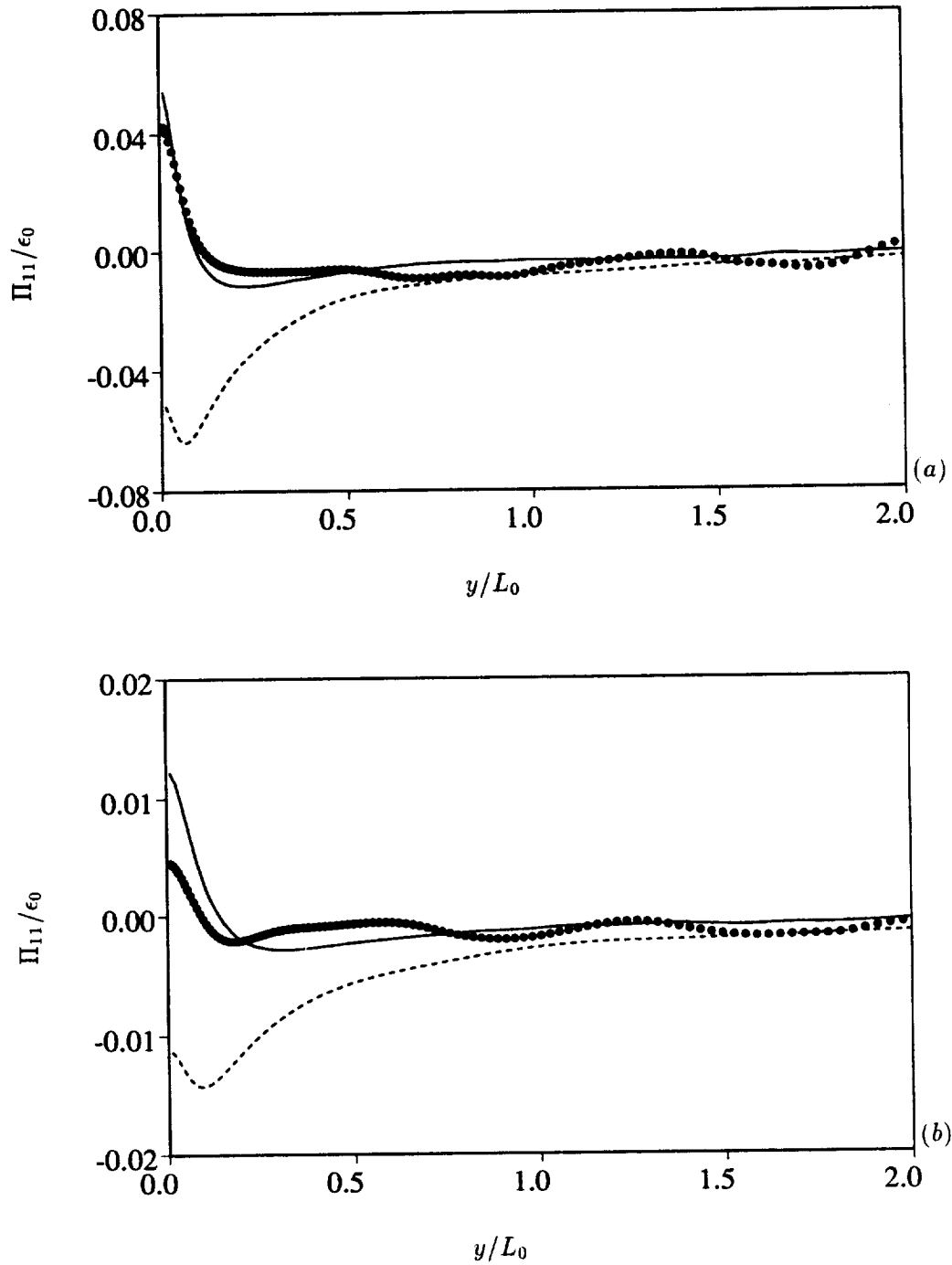
FIGURE 6. Pressure-strain near a free surface. $(Re_T = 134)$, (a) $t/T_0 = 1.0$, (b) $t/T_0 = 4.5$. ● , DNS data; - - - - , Rotta model; ———— , Present model.

3.3 Results

In the following test cases, there is only one independent pressure-strain term since $\Pi_{11} = -2\Pi_{22} = \Pi_{33}$, and all off-diagonal terms are zero. Figure 5a shows the performance of the model (equation 12) and the Rotta model ($\Pi_{ij} = -C_1 \epsilon a_{ij}$) in a shear-free wall flow at a Reynolds number of 134 (Perot & Moin, 1993). The direct numerical simulation (DNS) data is for the time $t/T_0 = 1.0$, where T_0 is the large eddy turnover time measured at the moment of boundary insertion. As previously mentioned, any model based on Reynolds stress anisotropy will have fundamentally incorrect behavior at the wall, so the more complicated variants of Rotta's model were not examined.

It can be seen that the present model, which includes the dissipation anisotropy, gives very good agreement with the DNS data. Figure 5b shows predictions for the same flow at a later time, $t/T_0 = 4.5$. The agreement of equation 12 ($C_\pi = 1.5$) with DNS data remains very good. The Rotta model not only has the wrong shape and has asymptotic behavior near the wall, but actually predicts the wrong sign of energy transfer near the wall.

The case of a free surface (Perot & Moin, 1993) is shown in figure 6a. The Reynolds number is 134, and the time is $t/T_0 = 1.0$. Again, the current model (with $C_\pi = 0.5$) shows good agreement with the data. Figure 6b shows the same simulation at a later time, $t/T_0 = 4.5$, and the model continues to be accurate. Because the pressure-strain term is smaller in the free surface case, the statistical and numerical noise is more apparent than in the shear-free solid wall case.

From these two cases and the case of homogeneous turbulence where C_π is typically taken in the range $1.5 - 1.8$, it appears that the coefficient C_π is not universally constant. This is not entirely surprising. It is reasonable that the two terms in the anisotropy equation (equation 10) might be proportional, but overly optimistic to expect that the constant of proportionality is fixed. In fact, Lumley (1987) has shown that the constant could be a function of the turbulent Reynolds number. As mentioned previously, we believe this model explicitly accounts for those Reynolds number effects, but the possibility for dependence on additional parameters still exists.

3.4 Summary

The pressure-strain model presented in this section was based on the anisotropy evolution equation for unsheared homogeneous turbulence, with generalizations to include the effects of inhomogeneity and two componentality near a wall. Although adjustment of the Rotta coefficient was required, this algebraic model for the pressure-strain produces surprisingly good results in the two test cases studied. Like the model for the dissipation, it is possible to think of this pressure-strain model as a combination of two terms, a near wall term (proportional to the anisotropy of the viscous terms) and a quasi-homogeneous far field term (proportional to the Reynolds stress anisotropy). This model breaks with tradition by not *only* using the Reynolds stress anisotropy in the model. This is a simple, yet vital step.

4. Turbulent transport model

4.1 Introduction

There is a high degree of similarity between the role of the triple correlations in the Reynolds stress equations and the role of the Reynolds stresses in the mean momentum equations. Both enhance transport, both become increasingly important as the Reynolds number increases, and both lead to fuller profiles in the respective statistical variables. For higher Reynolds number flows, where the gradients near the wall are very steep, it is particularly important to model the turbulent transport term accurately.

The modeling history of triple correlations is rather sparse. Most often, completely different physical effects such as viscous diffusion and pressure transport are lumped with turbulent transport. Such lumping is probably an unwise practice and will not be considered further in this section; it supposes that entirely different physical phenomena can be modeled collectively. Daly & Harlow (1970) used a gradient diffusion hypothesis for the triple correlations and proposed

$$T_{ijk} = C_s \frac{k}{\epsilon} R_{kl} R_{ij,l} \tag{13}$$

where a value of $C_s = .22$ was suggested by Launder & Morse (1979). Hanjalic & Launder (1972) noted that this model did not have the proper symmetry in its indices. They suggested

$$T_{ijk} = C_t \frac{k}{\epsilon} (R_{kl} R_{ij,l} + R_{jl} R_{ik,l} + R_{il} R_{kj,l}) \tag{14}$$

with $C_t = .11$. This more complicated expression can be derived from a simplification and modeling of the exact evolution equations for the triple correlations. More complicated expressions for the triple correlations also exist (Lumley 1984), but are not considered here since preliminary tests showed little difference with the Hanjalic & Launder model.

4.2 Modeling

Gradient transport models of the type mentioned above give only moderate to poor agreement in shear-free boundary layers. The problem with these models is not endemic to shear-free flows; Mansour, Kim & Moin (1988) witnessed equally poor performance in the case of fully developed channel flow. The clue to better modeling of the triple correlations is contained in the very first sentence of the introductory paragraph. The triple correlations should be modeled by using generalizations of low-order Reynolds stress models.

The simplest model for the Reynolds stress uses the eddy viscosity hypothesis. The eddy viscosity hypothesis works surprisingly well in a number of different flows. We might hope that an eddy viscosity hypothesis for the triple correlations might work as well, or perhaps even better, since higher order statistics tend to be more

uniform. The standard Hanjalic & Launder model (equation 14) can, in fact, be written in an eddy viscosity formulation,

$$T_{ijk} = C_t(\nu_{kl}^T R_{ij,l} + \nu_{jl}^T R_{ik,l} + \nu_{il}^T R_{kj,l})$$ (15)

where $\nu_{ij}^T = \frac{k}{\epsilon} R_{ij}$. The Hanjalic & Launder model is not usually viewed in this fashion; typically, it is justified as a severe simplification of the modeled triple correlation evolution equation. However, when viewed as an eddy viscosity model, there seems to be little justification for this choice of eddy viscosity. Instead, it is proposed that the eddy viscosity be a velocity scale times a length scale, as originally proposed by Prandtl in 1926. The previous section on dissipation modeling indicated that the generalized square root of the Reynolds stress tensor is an appropriate tensor velocity scale. So the following eddy viscosity is proposed, $\nu_{ij}^T = \overline{Q}_{ij} L_M$, where $\overline{Q}_{ik}\overline{Q}_{kj} = R_{ij}$ and L_M is a mixing length.

The wealth of literature on mixing length theory, originally developed for Reynolds stress modeling, can now be adopted at this higher level for the triple correlations. In this work, the mixing length will be assumed to be proportional to the large eddy length scale, $L_\infty = \frac{k^{3/2}}{\epsilon}|_\infty$, except close to walls or surfaces, in which case the mixing length is proportional to the distance from the wall. This choice of a mixing length, essentially due to Von Karman (1931), is simplistic. In complicated geometries, the distance to the wall is ill defined. It is not the goal of this section to evaluate mixing length models in detail, but to evaluate the modeling of the triple correlations and the turbulent transport term. It will be shown that this new method for defining the eddy viscosity improves turbulent transport models and is a promising direction to be moving in terms of triple correlation modeling.

The full eddy viscosity model for the turbulent transport terms then becomes

$$T_{ijk} = C_u L_M(\overline{Q}_{kl} R_{ij,l} + \overline{Q}_{jl} R_{ik,l} + \overline{Q}_{il} R_{kj,l})$$ (16)

where the constant C_u has been adjusted to a value of .18 and the mixing length is given by $L_M = (L^{-1} + y^{-1})^{-1}$, which gives a smooth transition between the near wall and far field limits.

4.3 Results

Figures 7a and 7b show comparisons of the models with direct numerical simulation (DNS) data from Perot & Moin (1994b). Figure 7a shows the tangential turbulent transport term for the case of a shear-free wall at a Reynolds number of 134 and time $t/T_0 = 1.0$. Figure 7b shows the normal turbulent transport term under identical conditions. The triple correlations take longer to converge than double correlations so there is some noise in the data, particularly far from the wall where turbulence length scales are largest. There is also some noise in the models from numerical differentiation.

The Daly & Harlow model captures the normal component well but overestimates the magnitude and position of the peak in the tangential component (it is, of course, also tensorally incorrect). The Hanjalic & Launder model captures the tangential
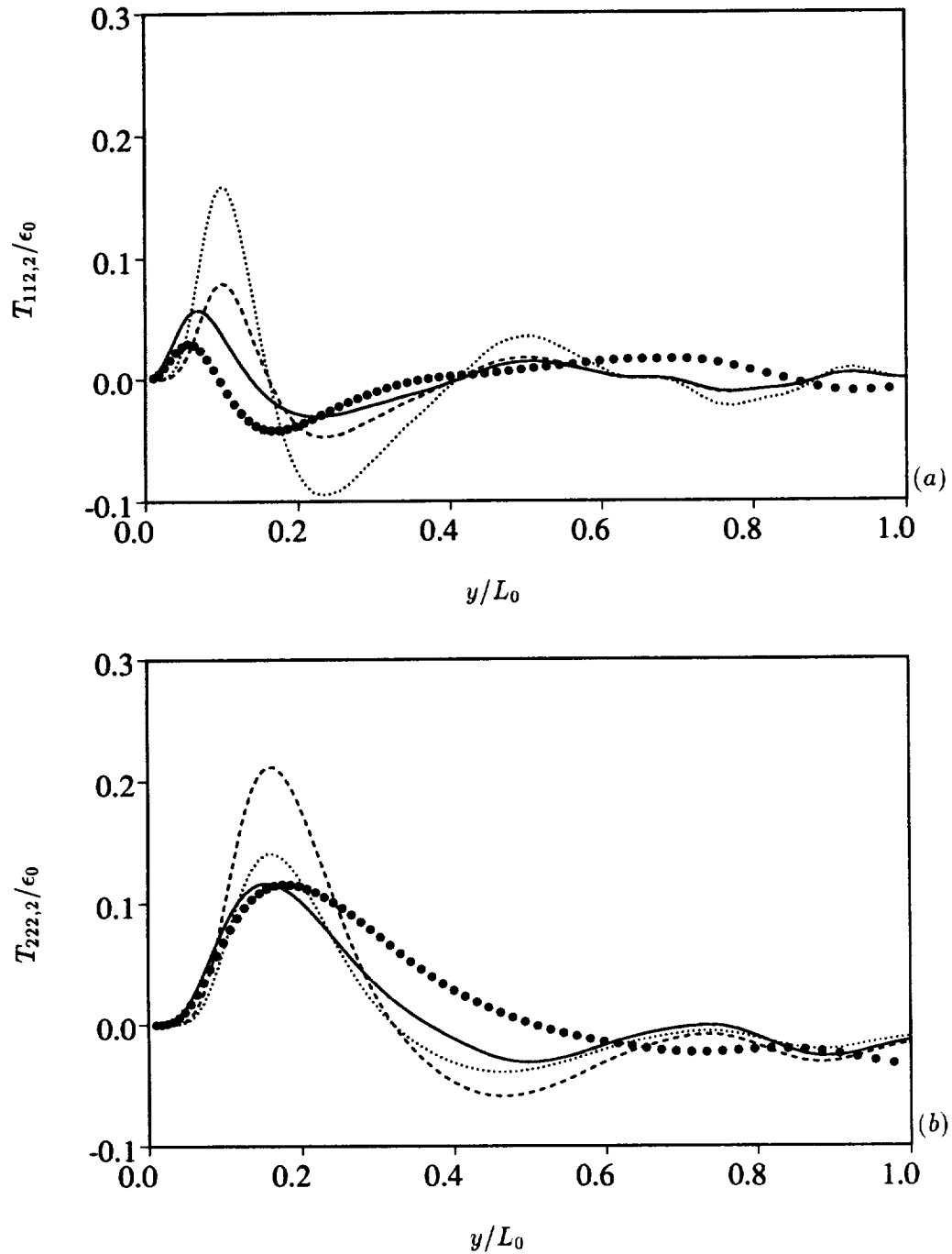
FIGURE 7.   Turbulent transport near a shear-free wall. (Re_T = 134) (t/T_0 = 1.0) (a) Tangential turbulent transport, (b) Normal turbulent transport.   ● , DNS data; ········ , Daly & Harlow model; ---- , Hanjalic & Launder model; ——— , Eddy viscosity model.

component better, but at the expense of overestimating the normal component. The eddy viscosity model gives better overall results than either of the previous two models. Similar results are shown for the shear-free wall case at a later time ($t/T_0 = 3.0$) in figures 8a and 8b. The conclusions remain the same.

The case of a free surface at a Reynolds number of 134 and time $t/T_0 = 1.0$ is shown in figures 9a and 9b. In this case, both the Daly & Harlow and the Hanjalic & Launder models overestimate the turbulent transport terms. The Daly & Harlow model is worse for the tangential component, and the Hanjalic & Launder model is worse for the normal component. Again, the eddy viscosity model gives better overall agreement with the DNS data. The eddy viscosity model tends to decay too quickly as one moves away from the wall, but this could easily be remedied by letting the $O(y)$ behavior in the mixing length persist farther into the flow.

It should also be mentioned that the eddy viscosity model has the right asymptotic behavior at the wall, whereas the standard models do not. Considering the simplicity of the eddy viscosity model and its relationship with an already well understood branch of turbulence modeling, and considering the fact that the eddy viscosity model gives similar or improved performance for these shear-free flows, it seems reasonable to recommend this approach in the future for triple correlation modeling.

4.4 Summary

One of the most obvious physical effects of turbulent flows is their increased ability to mix and transport flow quantities; eddy viscosity mimics this physical process. In this section, the Hanjalic & Launder model for turbulent transport was rewritten in an eddy viscosity formulation. An improved model for the triple correlations was developed, and good agreement with DNS data was achieved. Even better agreement with the DNS data could be achieved with improved and expanded definitions of the mixing length.

5. Conclusions

Near wall models for terms in the Reynolds stress evolution equations have been developed. These improved models perform well in the cases studies. The improvement shown by the models is based upon the inclusion of more physics into the modeling procedure. None of the models require additional constants over their quasi-homogeneous counterparts, and no *ad hoc* functions or *a priori* limiting behaviors have been imposed on the models.

Three fundamentally new concepts have been proposed in the context of this paper. The idea of decomposing the fluctuating velocity using a multiplicative decomposition into an intensity and a structure term led to an enhanced dissipation model. In terms of pressure-strain modeling, we have shown the efficacy of using the dissipation and diffusion anisotropy in conjunction with Reynolds stress anisotropy. Finally, we have suggested that the concept of eddy viscosity is useful at any modeling level when used to represent the effects of higher order correlations (in this case, triple correlations).
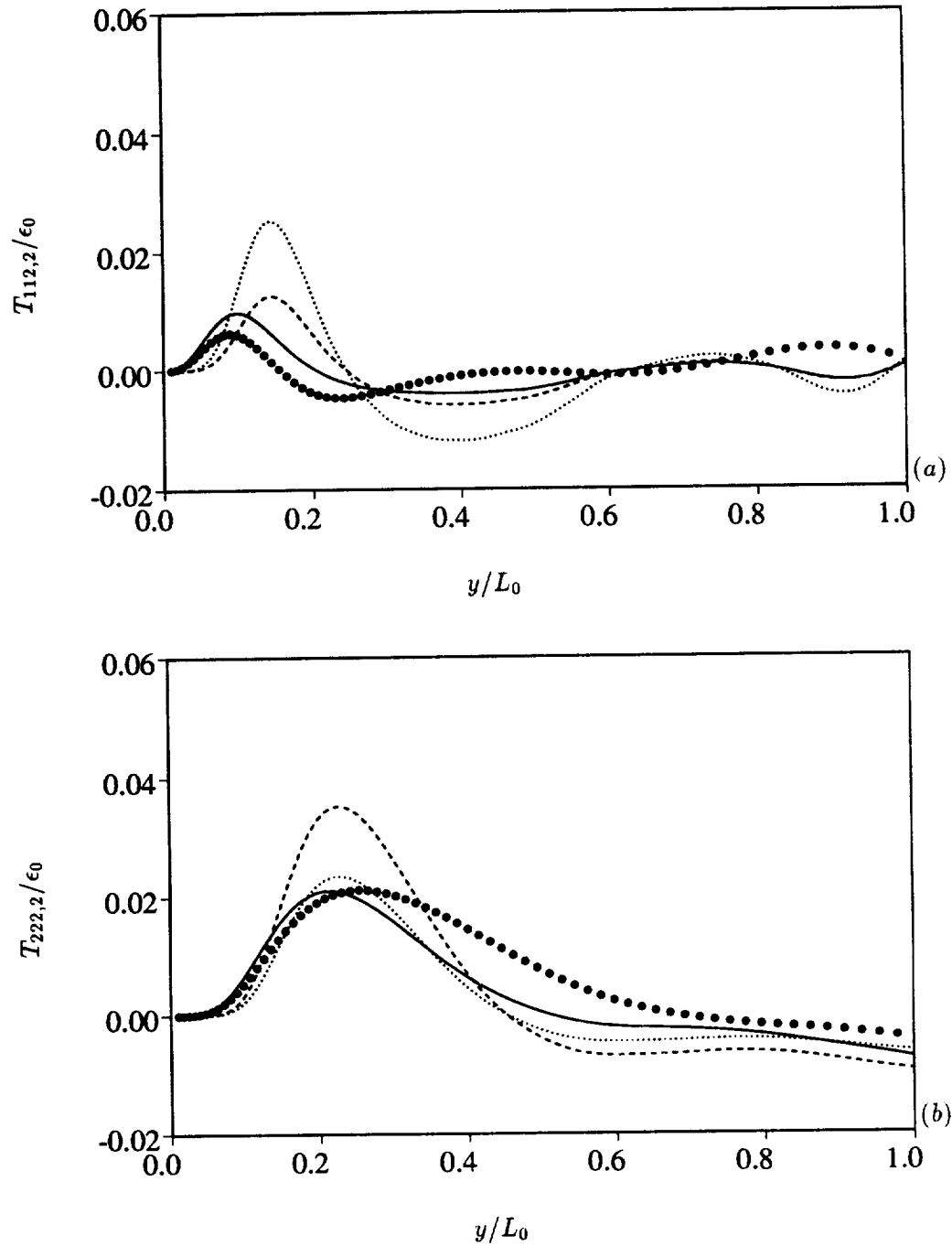
FIGURE 8.   Turbulent transport near a shear-free wall. $(Re_T = 134)$ $(t/T_0 = 3.0)$
(a) Tangential turbulent transport, (b) Normal turbulent transport.   ● , DNS
data; ········ , Daly & Harlow model; ---- , Hanjalic & Launder model; ——— ,
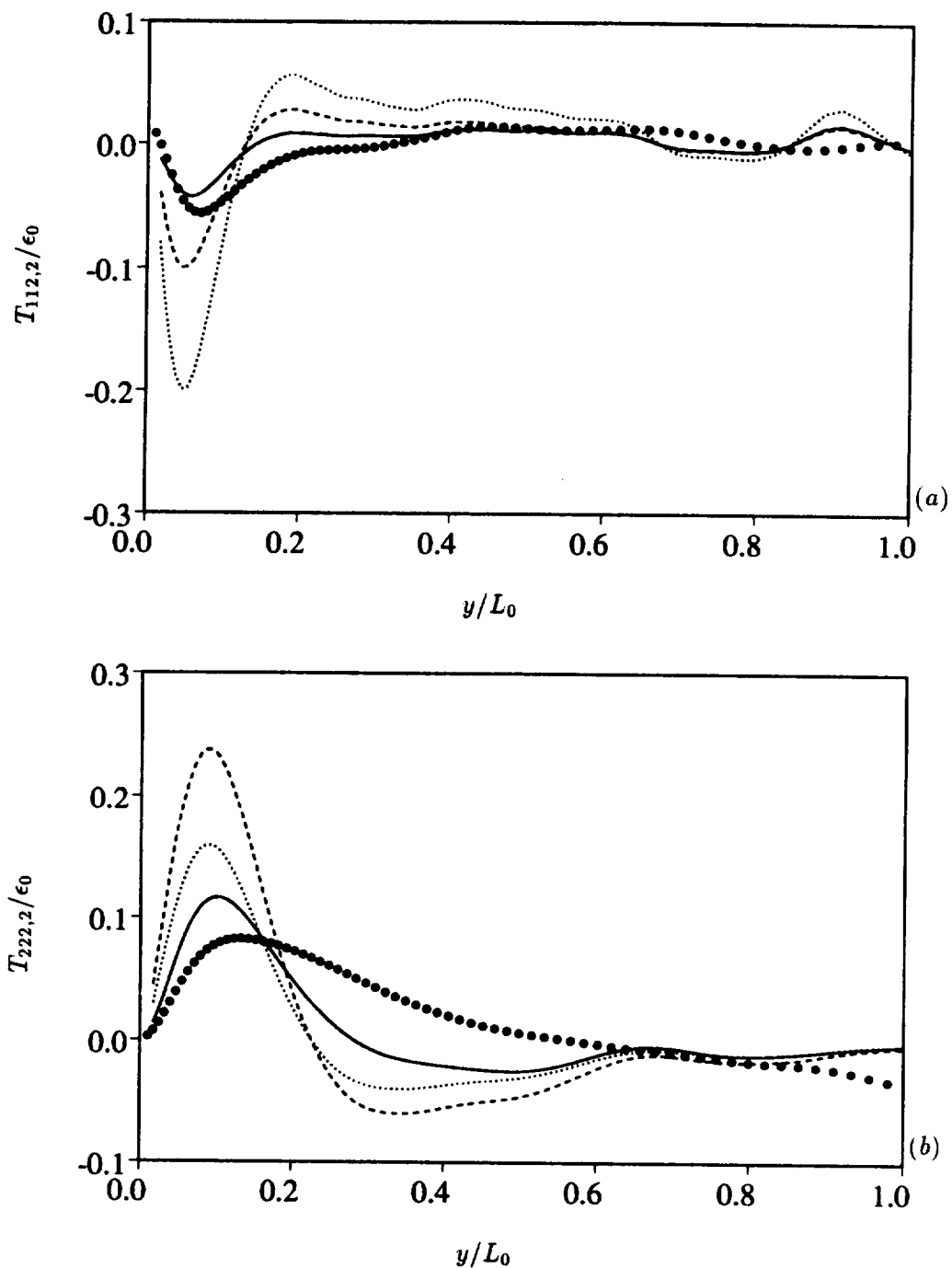Eddy viscosity model.

FIGURE 9. Turbulent transport near a free surface. ($Re_T = 134$) ($t/T_0 = 1.0$) (a) Tangential turbulent transport, (b) Normal turbulent transport. ● , DNS data; ········ , Daly & Harlow model; ---- , Hanjalic & Launder model; ——— , Eddy viscosity model.

REFERENCES

DALY B. J. & HARLOW F. H. 197 Transport equations in turbulence. *Phys. Fluids.* **13**, 2634-2649.

DURBIN, P. A. 1993 A Reynolds stress model for near-wall turbulence. *J. Fluid Mech.* **249**, 465-498.

HALLBACK, M. 1993 Development of Reynolds stress closures of homogeneous turbulence through physical and numerical experiments. *Ph.D. Thesis*, Dept. of Mechanics, Royal Institute of Technology, Stockholm.

HALLBACK, M. & JOHANSSON, A. V. 1992 Modeling of pressure-strain in homogeneous turbulence. *Advances in Turbulence 4*, TU Delft, Holland.

HANJALIC, K. & LAUNDER, B. E. 1975 Contribution towards a Reynolds-stress closure for low-Reynolds-number turbulence. *J. Fluid Mech.* **74**, 593-610.

KARMAN, T. VON 1931 *Proc. 3d Int. Congr. Appl. Mech.*, Stockholm pp. 85.

LAI, Y. G. & SO, R. M. C 1990 On near-wall turbulent flow modelling. *J. Fluid Mech.* **221**, 641-673.

LAUNDER, B. E., & MORSE, A. P. 1979 Numerical prediction of axisymmetric free shear flows with a Reynolds stress closure. *Turbulent Shear Flows I* (eds. Durst *et al.*), Springer Verlag, New York.

LAUNDER, B. E., REECE, G. J. & RODI, W. 1974 Progress in the development of a Reynolds-stress turbulent closure. *J. Fluid Mech.* **68**, 537-566.

LAUNDER, B. & REYNOLDS W. C. 1983 Asymptotic near-wall stress dissipation rates in a turbulent flow. *Phys. Fluids.* **26**, 1157-1158.

LUMLEY, J. L. 1978 Computational Modeling of Turbulent Flows. *Advances in applied mechanics*, C-S Yih, ed., Academic Press, New York, 123-176.

LUMLEY, J. L. & NEWMAN, G. R. 1977 The return to isotropy of homogeneous turbulence. *J. Fluid Mech.* **82**, 161-178.

MALAN, P. 1993 Heat transfer in shear-free turbulent boundary layers. *Report No. MD-64*, Department of Mechanical Engineering, Stanford University.

MANSOUR, N., KIM, J. & MOIN, P. 1988 Reynolds-stress and dissipation budgets in a turbulent channel flow. *J. Fluid Mech.* **194**, 15-44.

PEROT, J. B. & MOIN, P. 1993 Shear-free turbulent boundary layers: Physics and Modeling. *Report No. TF-60*, Department of Mechanical Engineering, Stanford University.

PRANDTL, L. 1926 *Proc 2d Int. Cong. Appl. Mech.*, Zurich, 62-75.

REYNOLDS, W. C. 1989 Effects of rotation on homogeneous turbulence. *Proceedings of the 10th Australasian Fluid Mechanics Conference*, University of Melbourne, Australia.

ROTTA, J. 1951 Statistical Theory of inhomogeneous turbulence. Part I. *Zeitschrift für Physik.* **129**, 257-572.

SCHUMANN, U. 1977 Realizability of Reynolds stress turbulence models. *Phys. Fluids.* **20**, 721-725.

SHIH, T. H. & LUMLEY, J. L. 1986 Second-order modeling of near-wall turbulence. *Phys. Fluids.* **29**, 971-975.

SPEZIALE, C. G., SARKAR, S. & GATSKI, T. B. 1991 Modeling the pressure-strain correlation of turbulence: an invariant dynamical systems approach. *J. Fluid Mech.* **227**, 245-272.

TSELEPIDAKIS, D. P. 1991 Development and application of a new second-moment closure for turbulent flows near walls. *Ph.D. Thesis*, Dept. of Mechanical Engineering, University of Manchester.